# On the Nature of Hops, Coordinates, and Detailed Balance for Nonadiabatic Simulations in the Condensed Phase

Maximilian F.S.J. Menger,<sup>†,‡</sup> Qi Ou,<sup>¶</sup> Yihan Shao,<sup>§</sup> Shirin Faraji,<sup>‡</sup> Joseph E. Subotnik,\*,<sup>∥</sup> and D. Vale Cofer-Shabica\*,<sup>∥</sup>

† Theoretische Chemie, Physikalisch-Chemisches Institut, University Heidelberg, INF 229, 69120 Heidelberg, Germany.

‡Zernike Institute for Advanced Materials, Faculty of Science and Engineering, University of Groningen, Nijenborgh 4, 9747AG Groningen, The Netherlands.

¶AI for Science Institute, Beijing 100084, China

§Department of Chemistry and Biochemistry, University of Oklahoma, Norman, Oklahoma
73019, United States

|| Chemistry, University of Pennsylvania, 231 S. 34 Street, Cret Wing 141D, Philadelphia,
Pennsylvania 19104-6243, United States

E-mail: subotnik@sas.upenn.edu; valecs@sas.upenn.edu

### Abstract

Photoinduced processes play a crucial role in a multitude of important molecular phenomena. Accurately modeling these processes in an environment other than vacuum requires a detailed description of the electronic states involved as well as how energy flows are coupled to the surroundings. Nonadiabatic effects must also be included in order to describe the exchange of energy between electronic and nuclear degrees of freedom correctly. In this work, we revisit the ring-opening reaction 1,3-cylohexadiene (CHD) in a solvent environment. Using our newly developed Interface for Non-Adiabatic Quantum mechanics/molecular mechanics in Solvent (INAQS) we trace the evolution of the reaction via hybrid quantum mechanics / molecular mechanics (QM/MM) surface hopping with a focus on the solvent's participation in the nonadiabatic relaxation process and the long-time approach to equilibrium. We explicitly include the MM solvent contribution to the nonadiabatic coupling vector—enabling an accurate approach to equilibrium at long times—and find that in highly multi-dimensional systems gradients can have little or nothing to do with the nonadiabatic couplings.

# Introduction

Photoinduced reactions are abundant in nature and play a role in a variety of important processes including photon-absorption during the initial step of photosynthesis, <sup>1</sup> energy conversion reactions, <sup>2</sup> and the conformeric changes of light-sensitive receptor proteins that enable humans to see their environment. <sup>3</sup> The understanding of these processes is valuable not only from an academic standpoint, but also to promote the development of more efficient technology, such as artificial light-harvesting systems. <sup>1,4–6</sup> To these ends, it is crucial that we understand the relaxation pathways available to the excited states of such systems so that we might learn how to hinder unwanted transitions or how to enhance desired routes.

Buoyed by recent software and hardware improvements, quantum chemistry has become

an important tool for the investigation of chemical processes. However to date—due to the unfavorable scaling of most electronic structure methods—a fully quantum chemical treatment is largely still limited to molecular systems composed of fewer than 100 heavy atoms, especially for molecular dynamics. While quantum mechanical studies of electronic relaxation are possible for isolated chromophores, it is generally not feasible to include the surrounding environment at the same level of theory. And yet, the environment may play a pivotal role in the underlying dynamical process: either by sterically restricting the system's motion, by perturbing the underlying electronic states, or by modifying the routes through which energy can flow out of (or into) the system. To include these environmental effects, hybrid Quantum Mechanics / Molecular Mechanics (QM/MM) simulations provide a good compromise between computational cost and accuracy. In most cases, the system is divided into 1) an active site (chromophore), where the photoinduced reaction occurs and which is treated at high level of electronic structure theory and 2) the remaining system, an environment, which is treated classically. Analyzing photoinduced processes requires modeling nonadiabatic effects (beyond Born-Oppenheimer) and tracking the flows of energy between molecule and environment and nuclei and electrons.<sup>7</sup>

To study nonadiabatic molecular dynamics in a complex environment, we have developed INAQS—the Interface for Non-Adiabatic Quantum mechanics/molecular mechanics in Solvent—which extends Gromacs (or other existing MD codes) to perform nonadiabatic dynamics (such as Fewest Switches Surface Hopping), utilizing an interface to the electronic structure code Q-Chem for performing QM/MM calculations under an electrostatic embedding. In a previous publication, we reported on the structure of the INAQS package and we demonstrated some of the package's more common features (absorption spectra, umbrella sampling, nonadiabatic dynamics) to study the ring-opening reaction of 1,3-cylohexadiene (CHD). In this paper, we will focus on the nonadiabatic, photoinduced dynamics of CHD using QM/MM surface hopping with particular attention paid to the inclusion of the solvent in the nonadiabatic dynamics. Focusing on electronic relaxation in the condensed phase, we

will analyze how the presence of a solvent leads to equilibration of a QM/MM system. In particular, we focus on answering the following questions:

- 1. Can we use short time hopping as a predictor of long-time branching?
- 2. What is the nature of the (often-ignored) nuclear-electronic coupling in solvent?
- 3. What are the implications of nonadiabatic coupling computed over system and solvent with respect to the approach to equilibration?

We note that while electronic properties like energies, gradients, wavefunction overlaps and nonadiabatic couplings are nowadays routinely computed in the framework of an electrostatic embedding, <sup>9–13</sup> to the authors' knowledge, the computation of nonadiabatic couplings on the MM sites are usually *not*. And so for the rescaling algorithm the question arises: which solvent atoms (or more generally, which MM atoms) contribute kinetic energy to the reservoir that dissipates the energy from a hop down or drives an electronic excitation upward? Different groups and packages <sup>12–15</sup> have answered this question in different ways, but largely by pre-selecting a set of "important" atoms in the system (in most cases only the QM atoms) and exclusively considering them for the rescaling algorithm; by contrast, IN-AQS employs Q-Chem's *ab initio* calculation of the nonadiabatic coupling vector on the MM atoms and rescales the momenta of all components of the system on equal footing. With a more accurate derivative coupling, one can then also ask: Can we use hopping as part of a reaction coordinate when modeling relaxation?

In this manuscript, we explore the answers to these questions. The remainder of this paper is organized as follows. First we review the theory of trajectory surface hopping and its extension to a QM/MM framework and outline computational details for our dynamics runs. The meat of our discussion then presents our results along with considerations of branching, the effects of working in a system with many (solvent) degrees of freedom, and some observations about the path towards equilibrium in terms of detailed balance. We conclude with a summary of our major findings.

# Theory

# Surface Hopping

Here, we provide a very brief review of trajectory surface hopping dynamics. <sup>16</sup> According to Tully's surface hopping approach, <sup>17</sup> the nuclei move on a single adiabatic potential energy surface, similar to Born-Oppenheimer molecular dynamics, but stochastic transitions between surfaces may occur as a function of the electronic degrees of freedom. The nuclear dynamics are defined by Newton's equations of motion:

$$\mathbf{M}\ddot{\vec{R}} = -\vec{\nabla}E_{\lambda},\tag{1}$$

where  $\vec{R}$  is the nuclear configuration vector,  $E_{\lambda}$  is the energy of the current active surface, and  $\mathbf{M}$  is the diagonal matrix containing the masses of all nuclei,  $m_{\alpha}$ :

$$(\mathbf{M})_{\alpha\mu,\beta\nu} = \delta_{\alpha\beta}\delta_{\mu\nu}m_{\alpha} \quad \alpha,\beta = \{1..N\} \; ; \; \mu,\nu = \{1,2,3\}.$$

There exist different flavors of surface hopping depending on how the hopping probability is computed. <sup>15,17–19</sup> INAQS adopts Tully's fewest switches algorithm (FSSH), <sup>17,18</sup> with several subtleties described in our previous paper. <sup>8</sup> The electronic degrees of freedom are propagated according to the time-dependent Schrödinger equation,

$$i\hbar \frac{\partial}{\partial t} \Psi(t) = \hat{H} \Psi(t),$$
 (2)

with  $\hat{H}$  the electronic Hamiltonian of the system and  $\Psi(t)$  the corresponding electronic wavefunction at time t. To solve this equation  $\Psi$  is typically expanded in a set of adiabatic basis functions  $\{\Phi_i\}$ ,

$$\Psi(t) = \sum_{i} c_i(t)\Phi_i(t). \tag{3}$$

Inserting the expansion (3) into the time-dependent Schrödinger equation (2) and integrating over the electronic degrees of freedom, yields the following equation of motion for the coefficients of the electronic wavefunction  $c_i$ :

$$i\hbar\dot{c}_i = \sum_j c_j \left[ V_{ij} - i\hbar\dot{\vec{R}} \cdot \vec{d}_{ij} \right],$$
 (4)

where  $V_{ij} = \langle \Phi_i | \hat{H}^{\text{elec}} | \Phi_j \rangle$  are the matrix elements of the electronic Hamiltonian, and  $\vec{d}_{ij} = \langle \Phi_i | \frac{\partial}{\partial \vec{R}} | \Phi_j \rangle$  are the nonadiabatic coupling vectors between adiabatic states  $\Phi_i$  and  $\Phi_j$ . As described in our previous paper, within INAQS, we do not require the calculation of the nonadiabatic coupling at every time step because we construct  $\dot{\vec{R}} \cdot \vec{d}_{ij} = \frac{1}{dt} (\log \langle \Psi(t) | \Psi(t+dt) \rangle)_{ij}$  in terms of the overlap of the wavefunction with itself at previous times—a source of considerable time-saving.

When a hop between adiabatic surfaces i and j occurs, the momenta are rescaled along the nonadiabatic coupling vector to conserve energy:

$$\vec{P}' = \vec{P} + \alpha \, \vec{d}_{ij} \quad ,$$

$$\alpha = -\frac{\vec{d}_{ij}^{\mathsf{T}} \mathbf{M}^{-1} \vec{P}}{\vec{d}_{ij}^{\mathsf{T}} \mathbf{M}^{-1} \vec{d}_{ij}} + \sigma (\vec{d}_{ij}^{\mathsf{T}} \mathbf{M}^{-1} \vec{P}) \left[ \left( \frac{\vec{d}_{ij}^{\mathsf{T}} \mathbf{M}^{-1} \vec{P}}{\vec{d}_{ij}^{\mathsf{T}} \mathbf{M}^{-1} \vec{d}_{ij}} \right)^{2} - \frac{2\Delta V}{\vec{d}_{ij}^{\mathsf{T}} \mathbf{M}^{-1} \vec{d}_{ij}} \right]^{1/2} \quad , \tag{5}$$

where the sign function  $\sigma(x) = -1$  if x < 0 and 1 otherwise, and  $\Delta V = E_j - E_i$ .

# QM/MM Surface Hopping

While trajectory surface hopping is a relatively computationally cheap scheme for nonadiabatic dynamics, it can only be applied to small and medium sized molecules due to the high cost of electronic structure calculations. To study larger systems and/or account for the effects of the environment, one typically turns to hybrid quantum/classical approaches.  $^{1,20-23}$ In QM/MM approaches the total energy of the system  $\mathcal{S}$ , can be written as the sum of the energy of the inner QM region  $\mathcal{I}$  treated at QM level of theory  $E_{QM}(\mathcal{I})$ , the energy of the outer environment  $\mathcal{O}$  treated at MM level of theory  $E_{MM}(\mathcal{O})$ , and their interaction,  $E_{QM-MM}(\mathcal{I},\mathcal{O})$ :<sup>21</sup>

$$E(\mathcal{S}) = E_{QM}(\mathcal{I}) + E_{MM}(\mathcal{O}) + E_{QM-MM}(\mathcal{I}, \mathcal{O}). \tag{6}$$

A variety of different QM/MM schemes have been developed,  $^{1,23,24}$  but for simplicity we restrict our discussion to mechanical and electrostatic embedding schemes, as these are implemented in INAQS. For mechanical embedding, the interaction term,  $E_{QM-MM}(\mathcal{I},\mathcal{O})$ , is specified by classical forcefield terms containing appropriate bonded and non-bonded interactions (Coulombic and Lennard-Jones). For electrostatic embedding, the classical charge-charge interactions between the MM atoms and the QM atoms are replaced by interaction between the MM charges and the QM electronic density via a nuclei-like 1-electron term in the electronic Hamiltonian:

$$\hat{H}^{QM-MM} = \sum_{\alpha} \frac{-Q_{\alpha}}{\left\| \vec{R}_{\alpha} - \hat{\vec{r}} \right\|},\tag{7}$$

where  $Q_{\alpha}$  is the charge of the MM atom  $\alpha$  at position  $\vec{R}_{\alpha}$  and  $\hat{\vec{r}}$  is the electron position operator.

Surface hopping for hybrid QM/MM schemes formally changes nothing as far as the propagation of the nuclear or electronic degrees of freedom; these quantities are propagated just as in vacuum simulations. The only difference now is that the properties—energies, gradients, derivative couplings, wavefunction overlaps—are computed within the QM/MM framework that includes the additional 1-electron term above and the nuclei are thus propagated on the adiabatic surfaces of the combined QM/MM system.

## Nonadiabatic Coupling Vector

Under a mechanical embedding, there is no polarization of the electronic density by the MM subsystem; thus there is no contribution to the nonadiabatic coupling from the MM system. However for an electrostatic embedding the picture changes: the electronic density now interacts with the MM environment through Eq. 7. Therefore, changes in the coordinates of the MM system can introduce a coupling between two electronic states.

The Hellmann-Feynman expression for the nonadiabatic coupling vector between states i and j with respect to nuclear coordinate  $\alpha$  is given by:

$$\vec{d}_{ij}^{\alpha} = \frac{\left\langle \Psi_i \middle| \vec{\nabla}_{\alpha} \hat{H} \middle| \Psi_j \right\rangle}{E_j - E_i}.$$
 (8)

Thus, taking the gradient of the electronic operator coupling the QM and MM regions (Eq. 7), we find the derivative coupling for the MM sites:

$$(E_j - E_i) \cdot \vec{d}_{ij}^{\alpha} = -Q_{\alpha} \left\langle \Psi_i \left| \frac{\vec{R}^{\alpha} - \hat{\vec{r}}}{\left\| \vec{R}^{\alpha} - \hat{\vec{r}} \right\|^3} \right| \Psi_j \right\rangle. \tag{9}$$

An implementation of Eq. 9 for configuration interactions singlets (CIS) and time-dependent density functional theory (TDDFT) and their spin-flip (SF) variants is available in Q-Chem 6.0.9 The relative contribution of the derivative coupling on the solvent and the implications of neglecting the MM components of the derivative coupling (especially with respect to the approach to equilibrium) will be discussed below.

# Methods

In our previous work, we presented INAQS, a new software package that enables the study of nonadiabatic molecular dynamics within a QM/MM framework, and demonstrated its application to the study of the ring-opening of 1,3-cyclohexadiene (CHD) to hexatriene (HT)

with umbrella sampling, spectra calculation, and nonadiabatic surface hoping dynamics. In this work we will revisit the CHD  $\rightarrow$  HT ring opening reaction, Scheme 1, but focus our attention exclusively on the nonadiabatic dynamics and the influence of the solvent on the relaxation process and highlight the impact of computing nonadiabatic coupling vectors on the solvent molecules.

Scheme 1: The ring-opening reaction of CHD proceeds by breaking the single bond between carbons 5 and 6.

The calculations follow our previous paper 8 and will only be briefly outlined. During dynamics, all properties were computed with the spin-flip variant <sup>25</sup> of TDDFT (SF-TDDFT) using the BHHLYP functional and cc-pVDZ basis set. Solvent parameters and equilibrated slabs were taken from Caleman et al. <sup>26</sup> Classical parameters for equilibrating CHD molecule were generated using Q-Force<sup>27</sup> at the cam-B3LYP/cc-pVDZ level of theory. The system was equilibrated by classical MD using the Gromacs software package for 2 ns. From the equilibration run, 51 independent configurations in each environment were selected for the trajectory surface hopping runs and were further relaxed via a 2 ps QM/MM equilibration to allow the system to adapt to the new Hamiltonian before the excited dynamics began. Following relaxation, all trajectories were well equilibrated with the exception of 8 trajectories in ethanol, where the internal energy of CHD was greater than 850K; these trajectories were excluded from further analysis. The 51 trajectories (less 8 for ethanol) were then propagated with nuclear time step 0.5 fs and electronic time step no greater than 0.025 fs for 500 fs. Velocity rescaling and reversal (Eq. 5) are computed using the nonadiabatic coupling vector on all atoms including solvent (Option 3 below). Other details of the surface hopping algorithm are given in our previous papers. 8,18

# Results

As shown in our previous work, the nonadiabatic ring-opening of CHD in vacuum computed via SF-TDDFT by INAQS correspond well to previous work at a higher level of theory (CASPT2/cc-pVDZ)<sup>28</sup> and show physically reasonable trends in the presence of ethanol and toluene solvents.<sup>8</sup> After photo-excitation to the bright S<sub>1</sub> state of CHD, the molecule relaxes to its ground state in approximately 200 fs after which either the closed CHD structure is retained or a ring-opening occurs and hexatriene (HT) is formed.

# Early-Time Hopping Structures and Dynamics as Predictors of Long-Time Branching

While the overall (long-time) dynamics described above are largely consistent in vacuum, toluene, or ethanol, a new set of information can be found by looking at the surface hopping trajectories in the vicinity of a hop. For ring opening systems like CHD, a natural reaction coordinate might be the length of the bond to be broken with a dividing surface at the saddle along that coordinate,  $R_{\text{c-c}}^{\dagger}$ . While one can consider the flux through such a surface to determine the rate of reaction, it isn't clear how to predict branching ratios. We then ask: do different solvents promote different hopping geometries and/or different short-time dynamics?

On the left-hand column of Fig. 1, we plot the distance between the 5th and 6th carbon atoms  $(R_{c-c})$  as a function of time. Note that the zero of time (t=0) is here taken to be the moment of the downward hop (where the molecule is near the conical intersection), after which the system commits to one of the wells on the ground state potential energy surface; the zero of time is *not* the time since excitation, decay from which occurs with a time constant of 40 fs in vacuum and 50 fs in either solvent. From this data, we can clearly see the two available reaction pathways: the molecule can either (i) relax into its vibrationally excited ground state remaining in the closed, CHD, conformation or (ii) the

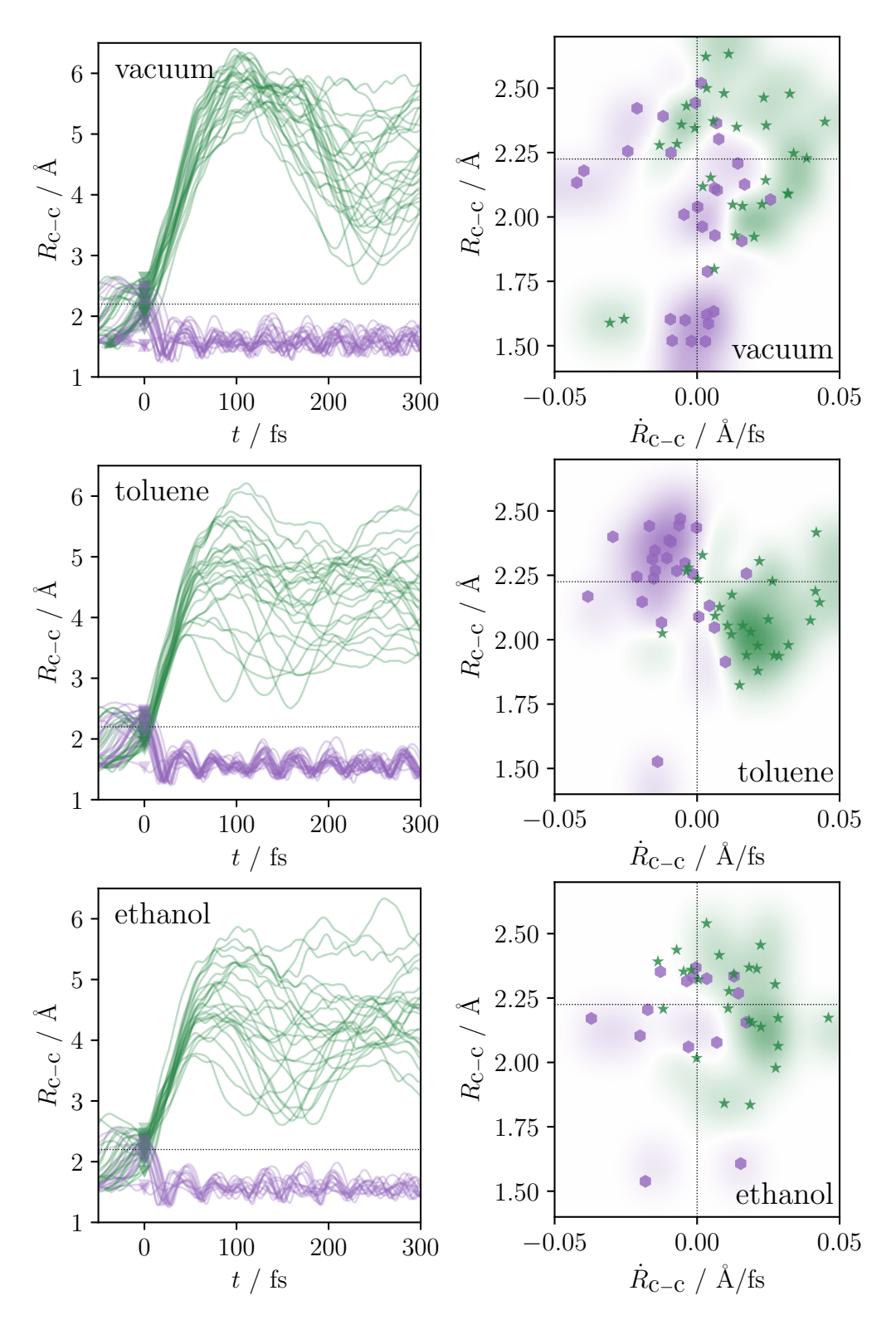


Figure 1: Left: time-series for  $R_{\rm c-c}$ , the single bond which may break, with t=0 taken as moment of the last downward hop. Green traces result in hexatriene; purple traces are unreactive. Right: phase-space plots showing the state of the system at the moment of a hop. Green stars represent trajectories that go to hexatriene and purple hexagons trajectories that remain in the cyclic form. Shaded regions are guides to the eye constructed via the difference of kernel density estimates for the two products. Dotted lines mark the saddle point  $(R_{\rm c-c}^{\ddagger}=2.2~{\rm \AA})$  along the minimum energy path and zero in velocity. Note that  $\dot{R}_{\rm c-c}$  at the time of a hop is much better than  $R_{\rm c-c}$  at the time of a hop as far as predicting the final outcome (CHD vs HT).

ring can open, breaking a C-C bond, to form the HT conformer. For both the vacuum and the solvent cases, no further conversion between HT and CHD is observed on the time scale of our simulation.

The main difference observed is among vacuum ring-opening trajectories' narrow distribution of C-C bond distances in the first 100 fs following excitation. According to the left hand side of Fig. 1, in solvent, the fluctuations of the reactive geometries over the first 200 fs after a hop are much more widely spread—suggesting steric hindrance in the presence of solvent. Moreover, we will see below that the distribution of geometries at the time of the hop for all product states is substantially broader in solvent than in vacuum —looking at not just the C-C bond distance but the overall structure. Given that there are clear differences in the rates at which the wavepackets diverge, one imagines that incorporating decoherence <sup>18</sup> into such a calculation would be important. We will address decoherence and its impact on surface hopping calculations for systems with many (solvated) degrees of freedom in a future publication.

More interesting than the left-hand side of Fig. 1 is the right, which shows a phase-space plot of the C–C bond length,  $R_{\text{c-c}}$ , against the velocity along the bond,  $\dot{R}_{\text{c-c}}$ , at the instant of a hop. As above, here we use the time of the hop as an additional degree of freedom to focus on a single time-slice of each trajectory: each point on the right represents an entire trajectory from the left taken at the time of the hop (t = 0).

One might expect that bond shortening ( $\dot{R}_{\rm c-c} < 0$ ) would lead to CHD and bond lengthening ( $\dot{R}_{\rm c-c} > 0$ ) would lead to HT. Indeed, the figures on the right of Fig. 1 indicate that velocity along the bond at the moment of the hop is a reasonable predictor of the long-time outcome of the reaction. For toluene-solvated CHD, the sign of the velocity at the time of the hop correctly predicts the outcome of the reaction in 85% of cases; for ethanol the fraction is 70%; the fraction is 59% in vacuum. The vacuum case can be significantly improved by including bond-length information: of hops with  $\dot{R}_{\rm c-c} > 0$  and  $R_{\rm c-c} > R_{\rm c-c}^{\ddagger}$ , 80% go on to form HT. Interestingly, for toluene,  $R_{\rm c-c}$  is a very poor predictor of the final outcome: at the

time of hopping, most reactive trajectories have small C-C separation relative to the saddle and most that revert to CHD are stretched. Fig. 1 therefore acts a strong caveat against using intuition to assert asymptotic dynamical behavior based on geometrical feature (e.g.  $R_{c-c}$ ).

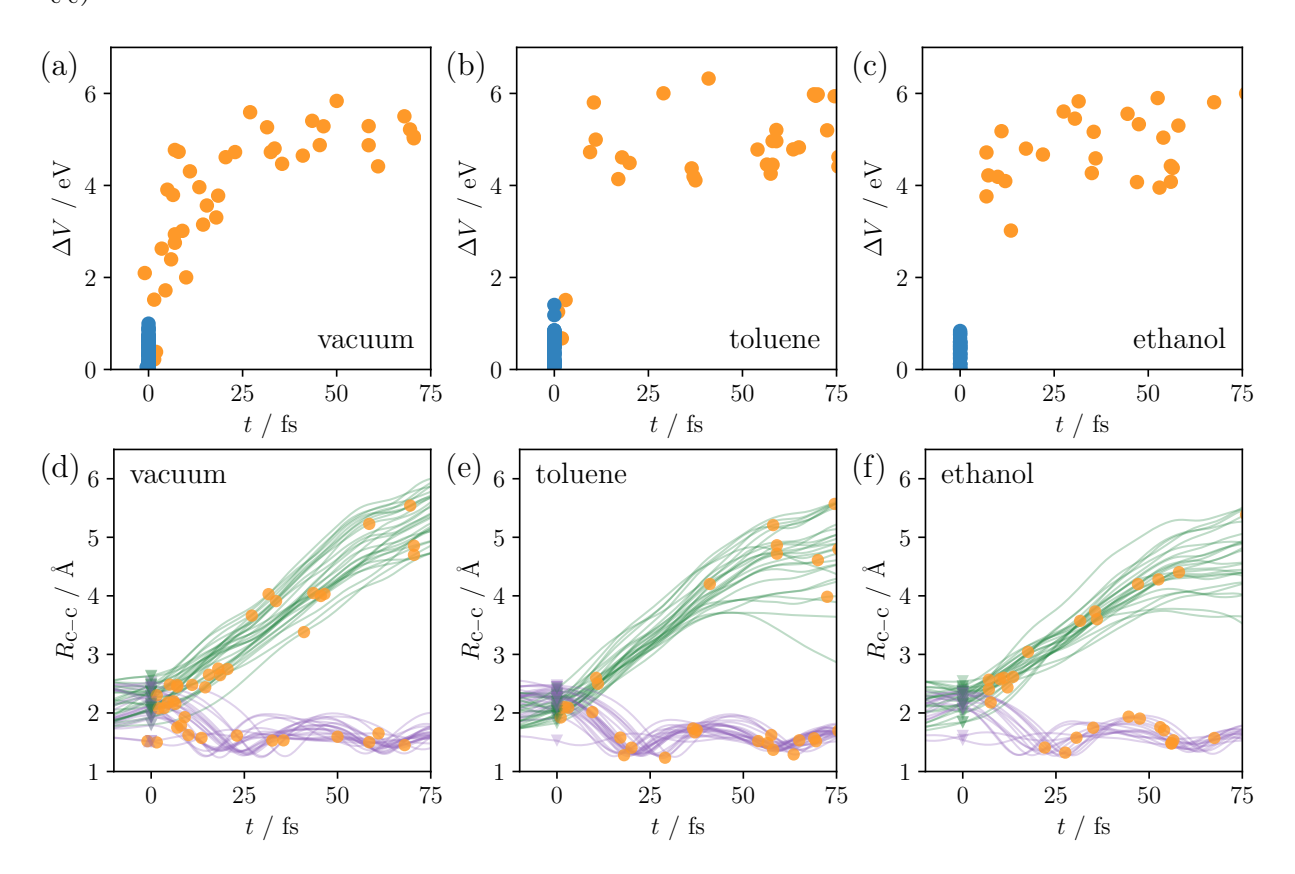


Figure 2: (a)–(c): Scatter plots showing the  $S_0$ – $S_1$  gap at time of a hop as a function of time since the last downward hop. Downward hops in are in blue and upward hops are in orange. (d)–(f): Traces of carbon-carbon bond length as time since downward hop. Plotted also are the (unsuccessful) attempted upward hops in orange. As in Fig. 1, reactive trajectories are colored in green and unreactive trajectories are in purple. For all three environments, the trajectories through phase space appear reasonably similar. The only meaningful difference is in panel (a), where we see that, in the vacuum case, there are far more frustrated hops at early times (and at small excitation energies), suggesting that solvent can play a subtle, non-obvious role in electronic relaxation.

To better understand the nature of how the short-time dynamics described above lead to branching, in Fig. 2 we plot the dynamics over the first 75 fs after a downward hop—this time as a function of the  $S_0$ – $S_1$  gap,  $\Delta V$ , and showing the frustrated hops that immediately follow. The upper panels show the energy gap at a frustrated hop as a function of time

and the lower panels show C-C separation as in Fig. 1. We see that after the downward hop, the system rapidly leaves the coupling region (small  $\Delta V$ ) independent of the ultimate product that will form (CHD or HT) and regardless of the presence of solvent. The major difference in the relaxation pathways available to CHD in solvent *versus* in vacuum appears in the first 20 fs following a downward hop (upper left panel). In this brief period, one can see that there are many attempted hops *upward*, back to S<sub>1</sub> with a smaller energy gap (less than 4 eV) than in the solvated systems or at later times (> 25 fs). These frustrated hops occur for 15 % of trajectories in vacuum but negligibly in either of the solvents.

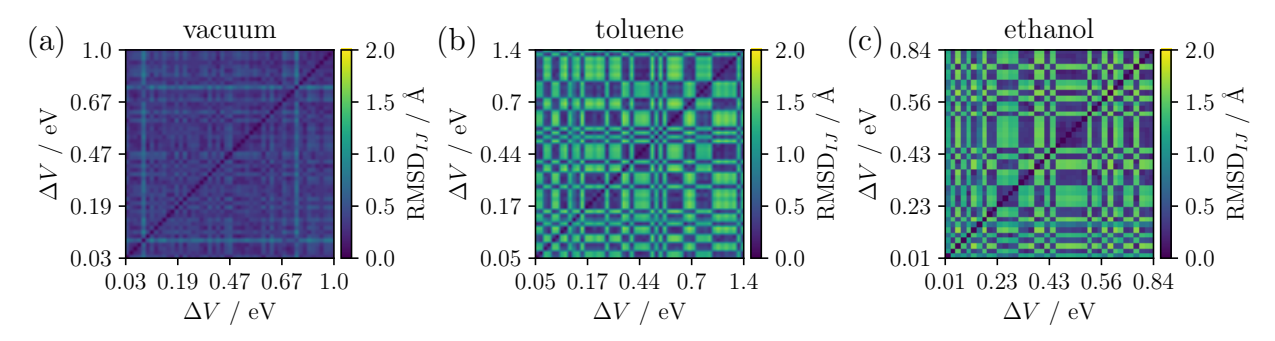


Figure 3: RMSD (for CHD only) between all structures at the time of a hop. Axes are sorted by energy gap and labels indicate range and 1st, 2nd, and 3rd quartiles. There is clearly more similarity between structures in the vacuum case indicating that the solvated structures span a greater region of configuration space.

In principle, the difference in the number and location of attempted hops could be caused by differences in the structures or in the electronic wavefunctions of the trajectories. That being said, while we observe nothing to implicate the wavefunctions differentially driving hopping, as shown in Fig. 3, we do observe that the region of configuration space visited by the system in solvent at the moment of a hop is much larger than when in vacuum. Mathematically, in Fig. 3, we quantify this larger sampled region in terms of the pairwise RMSD for all structures at the moment of a hop. For two structures, I and J, with N atomic nuclei located at  $\vec{R}_{\alpha}^{I}$  and  $\vec{R}_{\alpha}^{J}$ , the RMSD is:

$$RMSD_{IJ} = \min_{\mathbf{U}} \sqrt{\frac{1}{N} \sum_{\alpha}^{N} \left( \mathbf{U} \cdot \vec{R}_{\alpha}^{I} - \vec{R}_{\alpha}^{J} \right)^{2}}$$
 (10)

where the rotation matrix  $\mathbf{U}$  is chosen to maximally align the structures and minimize RMSD<sub>IJ</sub> (often by the Kabsch, but here by the QCP algorithm<sup>29,30</sup>). In the present work, we exclusively compare CHD structures, isolated from the solvent. We find the mean for all RMSD<sub>I $\neq J$ </sub> to be significantly smaller in vacuum, 0.377 Å, than in either solvent: 0.878 Å in toluene and 0.882 Å in ethanol. This finding is consistent with our previous observation that when calculating absorption, the primary influence of the solvent on CHD is enabling the exploration of a wider range of configuration space.<sup>8</sup> Altogether, the presence of solvent leads to a spreading out of trajectories through phase space and evidently the excited state potential energy surface is not characterized by strong, steep funnels to the conical intersection that would guide all trajectories to the same region following photoexcitation.

# Surface Hopping Dynamics in the Presence of Solvent

# The Nature and Utility of Derivative Coupling on Solvent atoms

Though Tully's original surface hopping scheme was implemented on one-dimensional model problems, much richer photodynamics emerges for multidimensional problems (even if exact benchmarking is impossible). In such a case, energy dissipation and barrier crossing become much more realistic and, at the same time, nonseparable. One of the conceptual breakthroughs in the FSSH algorithm was the notion that all nonadiabatic crossing events should rescale momentum in the direction of the derivative coupling, a notion that goes back to Pechukas<sup>31</sup> and was later confirmed by Herman<sup>32</sup> and is clearly implicated within the quantum-classical Liouville equation (QCLE). <sup>33–35</sup> In practice, however, calculating a multi-dimensional nonadiabatic coupling vector is non-trivial and, for many calculations (especially QM/MM calculations), modern codes often make approximations.

1. The simplest scheme (and most aggressive approximation) is to simply rescale along the unprojected momentum vector of the whole system. While this method is attractive because it is trivial to implement and does not require the calculation of the nonadi-

abatic coupling, one expects it to be successful only in situations where the dynamics are dominated by a single degree of freedom and/or the velocity and nonadiabatic coupling vectors are coincident. For small systems, where the total molecular system is involved in the process this technique can lead to acceptable results. <sup>13–15,36</sup>

- 2. While unprojected rescaling may succeed in vacuum, QM/MM calculations can easily involve many (thousands) degrees of freedom of which surely not all are relevant to the nonadiabatic relaxation. Simply including the kinetic energy of all the atoms (solvent + chromophore) for rescaling would functionally provide an infinite energy bath and no hops would be frustrated. We know that frustrated hops are important to the approach to equilibrium <sup>37,38</sup> and their neglect would lead to severe artifacts by driving electronic energy into the QM region. Masking algorithms, which require the user to pre-select the atoms for rescaling, usually the QM atoms, have been previously used to avoid these non-physical effects. <sup>12,13</sup> However, atom-selection must be done with great care especially if extending beyond the QM region. While it may be desirable to study the solvent's influence on the nonadiabatic process, as we will explore below, it is not clear that it is even possible to successfully balance the requirements of frustrating some hops and promoting others which are physically relevant to the reaction.
- 3. A third option is to simply follow Pechukas' (and the QCLE's) prescription and use only the part of the kinetic energy that arises from momentum parallel to the nonadiabatic coupling vector for rescaling. An expedient approximation—arising from the fact that most electronic structure codes compute the nonadiabatic couplings exclusively on the QM region—is to ignore the MM atoms for rescaling. To the extent that solvent do not participate in the process, using the nonadiabatic coupling has the advantage that it gives an *ab initio* criterion for selecting the QM atoms relevant for rescaling.

One of the novel features of our implementation of QM/MM surface hopping is the inclusion of the nonadiabatic coupling vector on all solvent molecules, which enables calculating

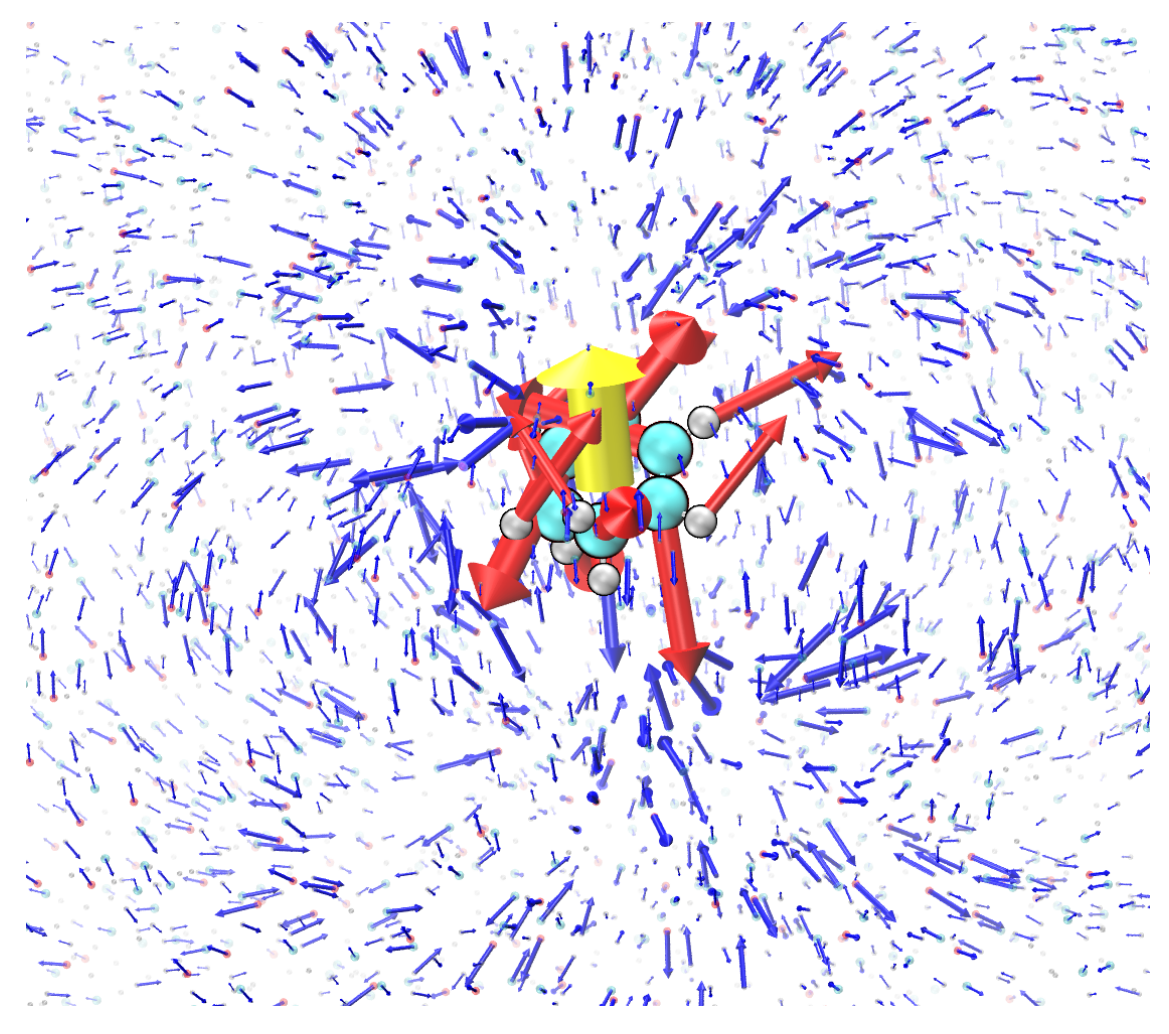


Figure 4: Nonadiabatic coupling vector between  $S_0$  and  $S_1$  rendered on the solvent (blue) as as well as CHD (red). The relative magnitude of vectors is indicated by the volume of the arrows. The transition dipole moment,  $\langle S_0 | \vec{X} | S_1 \rangle$ , is plotted in yellow. The long range behavior of the nonadiabatic coupling is of a dipole field, see Eq. 9.

the participation of the environment in the nonadiabatic process. The Hellman-Feynman expression for the nonadiabatic coupling vector for solvent atoms under an electrostatic embedding QM/MM scheme is given in Eq. 9 and implemented in Q-Chem 6.0.9 In Fig. 4 we visualize the nonadiabatic coupling on the solvent (blue arrows) as well as on CHD (red arrows). During a hop, the momenta of all atoms in the system are scaled along the nonadiabatic coupling vector. Frustrated hops, which are numerous during relaxation, similarly reverse the momentum of all atoms along the nonadiabatic coupling according to the Jasper and Truhlar's usual criterion. <sup>39</sup> While the absolute magnitude of the nonadiabatic couplings are usually much smaller on solvent atoms than on CHD, they are not negligible and still impart non-trivial momentum. As we discuss below the overlap between the nonadiabatic coupling and the gradient is minimal in this condensed phase system, highlighting the multidimensional nature of current problem.

To illustrate the sensitivity of the selection criteria discussed above (see Option 2) as far as determining the outcome of a surface hopping direction, in Fig. 5 we plot the fraction of frustrated hops that is recovered when rescaling momenta using the N nearest solvent molecules and rescaling in the direction of the instantaneous momenta. The denominator here is the number of frustrated hops recovered when running dynamics and rescaling with a proper derivative coupling. According to Fig. 5, if one includes the first two solvation shells (N=12), there is enough kinetic energy available so to allow all upward hops in the toluene case. For ethanol (the smaller molecule) N=12 corresponds to 50% of the frustrated hops being incorrectly allowed. Agreement with rescaling along the nonadiabatic coupling vector is obtained for small numbers of solvent (i.e. the fraction is unity when N is small), but clearly no such rule of thumb can hold in general. In the present case, CHD is only weakly coupled to the solvent but for systems where there is more charge rearrangement during the nonadiabatic transition,  $^{40}$  clearly choosing the "correct" N would be impossible and not practical.

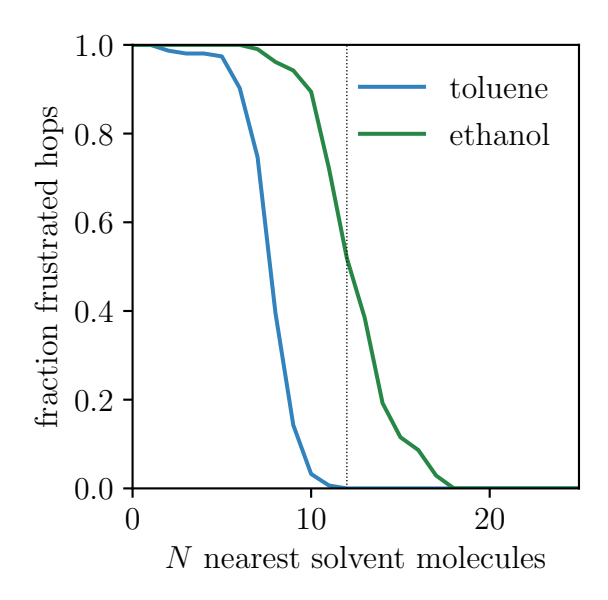


Figure 5: A demonstration of the importance of choosing the correct momentum rescaling direction. Here, we quantify the impact of hypothetically rescaling momenta in the direction of the instantaneous momentum (rather than the derivative coupling) for both the CHD nuclei and a small number (N) of solvent molecules closest to the QM system. On the y-axis, we plot the number of such hypothetically frustrated hops divided by the number of hops we recover when using a proper rescaling along the derivative coupling. If we include only a few solvent molecules, there are far more frustrated hops, indicating that an arbitrary cutoff would need to be applied in this case; there are clearly inherent dangers to using the instantaneous momentum rather than the derivative coupling when rescaling momenta in the condensed phase. The dashed line at N=12 represents that set of all nearest neighbors.

## Multi-dimensional Aspects of Surface Hopping

For 1-dimensional surface hopping models, one assumes that all electronic dynamics are dependent on only a single nuclear reaction coordinate. However, in a real system, there are often multiple relevant degrees of freedom. Is it reasonable to expect the directions breaking adiabaticity to have anything to do with the direction advancing the reaction? In general the answer is decidedly no.

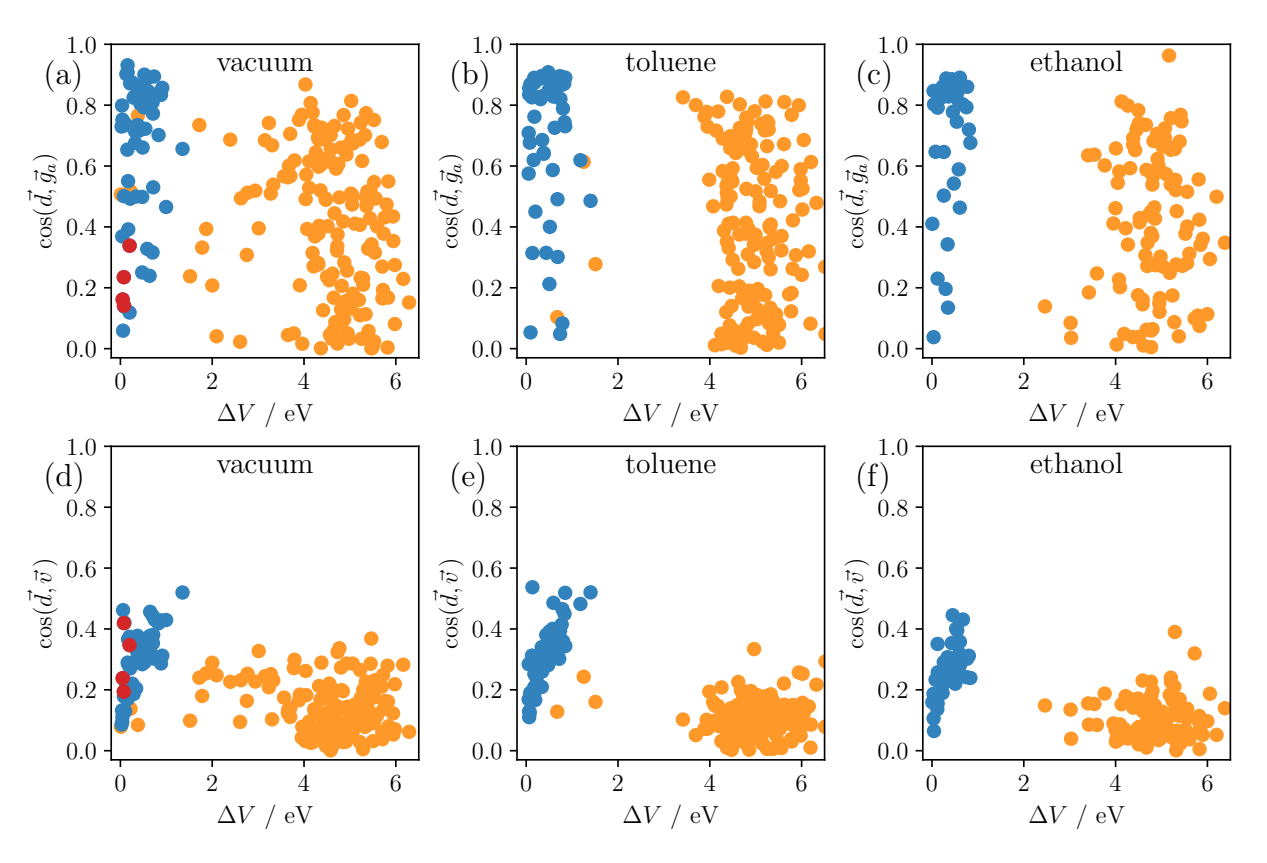


Figure 6: (a)–(c): Scatter plots of cosine of the angle between the nonadiabatic coupling vector,  $\vec{d}$ , and the difference in the gradients,  $\vec{g}_a$ , as a function of adiabatic energy gap. Downward hops in are in blue and upward hops are in orange (frustrated) or red (successful). The gradients do not generally align with the nonadiabatic coupling, highlighting the multidimensional nature of the problem. (d)–(f): Hops by the cosine of the angle between the nonadiabatic coupling vector and the nuclear velocity,  $\vec{v}$ , as a function of the S<sub>0</sub>-S<sub>1</sub> gap. We consider only the portion of the nonadiabatic coupling that extends over CHD. In the solvated systems the nonadiabatic coupling vector on solvent molecules is effectively uncorrelated with their velocities, *i.e.*  $\cos(\vec{v}_{\text{solvent}}, \vec{d}_{\text{solvent}}) \approx 0$ .

For a two-level system, the directions in the nuclear configuration space that are most

relevant to the electronic state are defined by the nonadiabatic coupling vector,  $\vec{d} = \vec{d}_{01}$  (c.f. Eq. 8), and the gradient of the difference in the energy levels,  $\vec{g}_a$ ,

$$\vec{g}_a = \vec{\nabla}\mathbf{S}_1 - \vec{\nabla}\mathbf{S}_0. \tag{11}$$

To the extent that these directions are coincident, a system will be well described by a single coordinate. In the upper panels of Fig. 6, we consider the correlation between  $\vec{d}$ , and  $\vec{g}_a$ ,

$$\cos(\vec{d}, \vec{g}_a) = \frac{\vec{d} \cdot \vec{g}_a}{\|\vec{d}\| \cdot \|\vec{g}_a\|}.$$
(12)

While the majority of successful hops have  $\vec{g}_a$  roughly in the same direction as  $\vec{d}$ , there are many where they are nearly orthogonal. That is, there are many times when the system traverses the conical intersection such that  $\vec{g}_a$  and  $\vec{d}$  have little to do with each other. For frustrated hops, there's a roughly uniform distribution of cosines, suggestive of no correlation at all.

Continuing to explore the multi-dimensional aspects of this system, in the lower portion of Fig. 6 we turn our attention to correlations between the velocity,  $\vec{v} = \dot{\vec{R}}$ , and the derivative coupling. The  $\vec{d} \cdot \vec{v}$  term in the equations of motion for the electronic wavefunction (Eq. 4) is responsible for driving transitions between adiabatic states. In Fig. 6(d)–(f), we make a scatter plot of the cosine of the angle between the nonadiabatic coupling vector and the velocity for each hopping (or attempted hopping) event. For successful downwards transitions (in blue), there appears to be some correlation between the angle and the energy gap, with greater coincidence at larger gaps. On the one hand, these two vectors are never parallel and are often orthogonal during the long equilibration period that follows the return to the ground state (orange frustrated hops in at large gap); this fact highlights the very multidimensional nature of the problem. That being said, on the other hand, it is remarkable that  $\vec{d}$  and  $\vec{v}$  almost always have an angle larger than  $\pi/3$  between them, i.e.  $\cos(\vec{d}, \vec{v}) \lesssim 0.5$  during a hop down, suggesting that there clearly exist reduced reaction coordinates with some meaning

for this solvated system. Note that we only consider the nonadiabatic coupling and velocity on CHD; in an extended system, the velocities of distant solvent molecules will necessarily be uncorrelated with the nonadiabatic coupling.

# Energy Dissipation: The Path Towards Equilibrium in a Condensed Environment

Following photoexcitation in the presence of a solvent, one would like to understand how the energy is dissipated by the environment and how those energetic pathways modify the course of the reaction. For QM/MM surface hopping, two primary energy dissipation mechanisms exist:

- 1. The first pathway is via simple collisions, mediated by non-bonded interactions. For CHD, the presence of solvent drives the system to a explore a larger region of configuration space (see Fig. 3), which leads to the spreading of energy (which can be captured by the broadening of the simulated UV spectrum<sup>8</sup>). Energy transfer in this fashion is slow and effectively diffusion limited.
- 2. The other pathway is the instantaneous interconversion of electronic and kinetic energy at the moment of a hop. Energy conservation demands that, during a hop between adiabatic energy surfaces, potential energy be exchanged with kinetic energy. If MM atoms are included in the momentum rescaling scheme, as they are here, then a unique pathway for the energy transfer between QM and MM sites opens. Exactly where and how this energy is deposited or drawn from may influence the resulting dynamics and approach to equilibrium. As the rescaling method plays such a fundamental role in partitioning energy, an inaccurate treatment may lead to non-trivial errors in the simulation.

To investigate the relative importance of the solvent contribution to momentum rescaling, in Fig. 7 we plot the per-atom momentum transfer during a successful hop as a function of

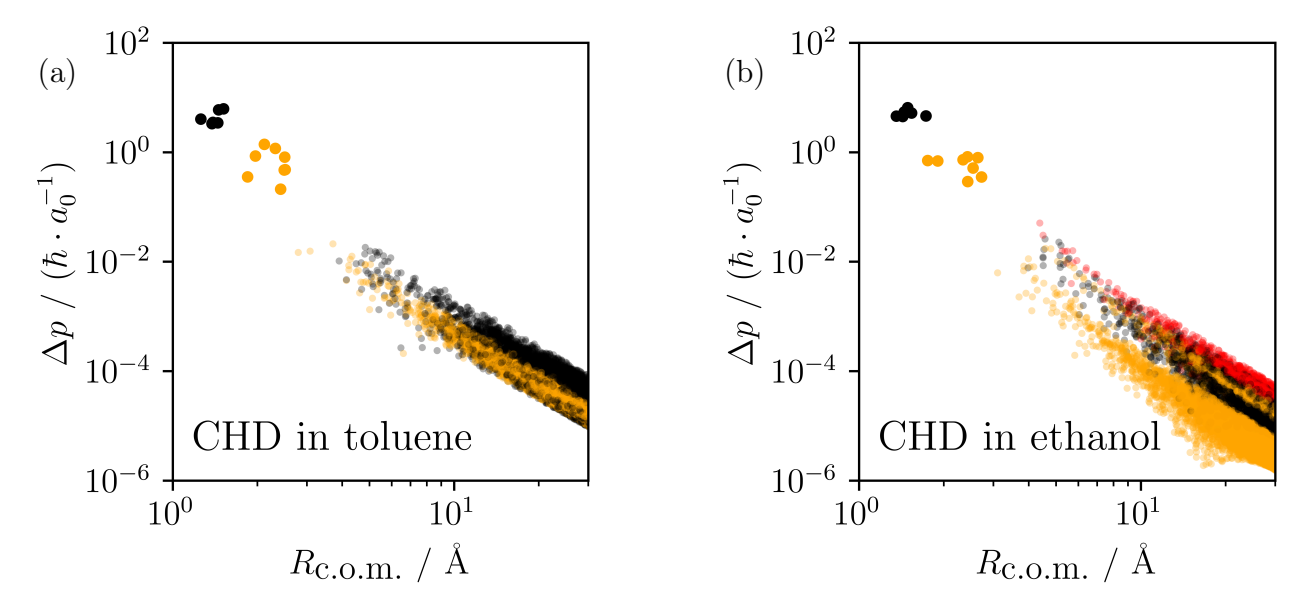


Figure 7: Per-atom momentum transfer in atomic units as a function of distance from CHD center of mass for representative successful downward hops in toluene (a) and ethanol (b). Black=Carbon, Orange=Hydrogen, Red=Oxygen. The larger circles in the upper left of each panel are the atoms composing CHD, the smaller symbols represent solvent atoms. Note that although every individual solvent atom absorbs only a small amount of momentum transfer, altogether the solvent does take on a significant amount of transfer simply because there are so many solvent molecules.

distance from the CHD center of mass for typical hops in toluene and ethanol. The nearer atoms, with largest momentum transfer make up CHD and the more distant ones the solvent. For the kth atom,

$$\Delta p_k = \|\vec{p}_k - \vec{p}_k'\|$$

where  $\vec{p_k}$  and  $\vec{p_k}'$  are the momenta before and after the hop respectively, the latter found by solving the energy conservation equations for momentum rescaling, Eq. 5.

As one can see from Fig. 7 there is a clear hierarchy of contributions split between three distinct regions in either solvent. The carbon atoms on CHD show the largest momentum change, followed by the CHD hydrogen atoms; lastly the atoms of the solvent appear as a continuum. Solvent atoms generally experience 2-3 orders of magnitude smaller momentum transfer than the atoms in CHD. This difference is not surprising as CHD has relatively weak coupling to the solvent and thus the nonadiabatic coupling on the solvent atoms is relatively

small. However, and despite the considerably smaller per-atom effect, the total momentum transfer to the solvent,  $\Delta p^{\text{solvent}} = \sum_{k \in \text{solvent}} \Delta p_k$ , usually represents between 2% and 8% of the total and in some instances is as much as 16%. We expect that for polar species or for a system with charge transfer states, the coupling and therefore momentum transfer will be larger.

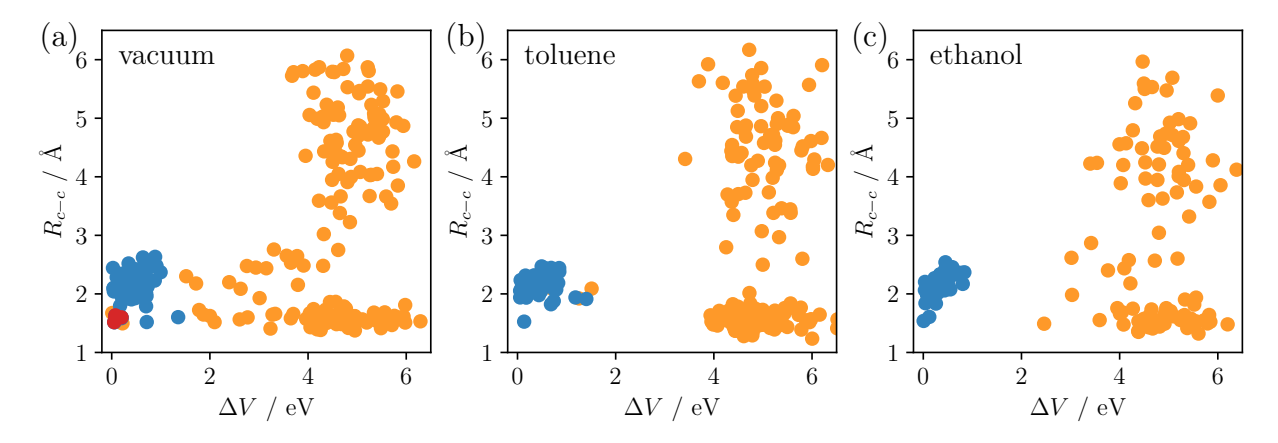


Figure 8: Scatter plots showing C-C bond distance as a function of energy the  $S_0$ - $S_1$  gap at time of a hop. Downward hops in are in blue and upward hops are in orange (frustrated) and red (successful). Frustrated hops can arise even with very large energy gaps (as large as 6 eV) and clearly are essential for maintaining detailed balance.

To further analyze the energy dissipation via the hopping mechanism, in Fig. 8 we plot hops down (blue) and up (orange when frustrated and red when successful) by C–C separation and energy gap. With the exception of 4 successful hops up in 2 trajectories in vacuum, upward hops are all frustrated. The relatively tight distribution for hops downward stands in contrast to the distribution for upward, frustrated hops, which span a larger range of energies and C–C separations. At small  $R_{\rm c-c}$ , the hops are initiated from CHD and at larger distances, from hexatriene. Notably many frustrated hops appear for high energy gaps ( $\Delta V > 2$  eV) highlighting the importance of physically meaningful selection of the relevant atoms for the rescaling scheme. Most trajectories fall out of the region of the conical intersection relatively quickly (see Fig. 2), but in vacuum, there are some trajectories that persist in the region of small gap, a feature we explored in Fig. 3.

Altogether, Fig. 8 shows how energy transfer and the dissipation of energy among many

degrees of freedom is ultimately the cause that leads to the presence of frustrated hops in a solvated environment, the phenomenon by which surface hopping maintains detailed balance. <sup>37,38</sup>

# Conclusion

We have presented the nonadiabatic relaxation dynamics of 1,3-cyclohexadiene in vacuum, toluene, and ethanol as computed via explicit QM/MM with electrostatic embedding. We analyzed the short and long-time dynamics and made a few limited conjectures about how short-time hops can translate into long-time populations for this photochemical process. We implemented and plotted the nonadiabatic coupling vector on the MM sites for electrostatic embedding. This analysis allows one both to gain intuition as to the role of solvent as far as facilitating a nonadiabatic transition as well as potentially helping to define the relevant separation of QM and MM atoms. By computing the nonadiabatic coupling vectors on the solvent atoms, we have also been able to explicitly include the solvent in the electronic relaxation in an ab initio fashion so as to ensure that the correct equilibrium (with detailed balance) is achieved at long times. We find that in highly multi-dimensional systems the gradients can have nothing to do with the nonadiabatic couplings.

Looking forward, the case of CHD is the simplest possible model QM/MM problem because no charge transfer occurs and the system-solvent interaction is weak. In particular, the hopping dynamics are largely dictated by the chromophore (even though hops up are gated by solvent). To that end, the next step of this research is clearly to work with problems of charge transfer and large (unshielded) charges. In such situations, we anticipate that systems with stronger solute-solvent interaction will enhance the electronic effects substantially.

# Acknowledgement

This work was supported by the U.S. Air Force Office of Scientific Research (USAFOSR)

(under Grant Nos. FA9550-18-1-0497 and FA9550-18-1-0420) and the National Science Foundation (under Grant No. CHE-2102071). MM and SF thank the Innovational Research Incentives Scheme Vidi 2017 with project number 016. Vidi. 189.044, which is financed by the Dutch Research Council (NWO), for their funding. We thank the DoD High Performance Computing Modernization Program for computer time.

# References

- (1) Curutchet, C.; Mennucci, B. Quantum Chemical Studies of Light Harvesting. *Chem. Rev.* **2017**, *117*, 294–343.
- (2) Goyal, P.; Hammes-Schiffer, S. Role of solvent dynamics in photoinduced proton-coupled electron transfer in a phenol–amine complex in solution. *The Journal of Physical Chemistry Letters* **2015**, *6*, 3515–3520.
- (3) Yang, X.; Manathunga, M.; Gozem, S.; Léonard, J.; Andruniów, T.; Olivucci, M. Quantum-classical simulations of rhodopsin reveal excited-state population splitting and its effects on quantum efficiency. *Nature Chemistry* **2022**, *14*, 441–449.
- (4) Jones, C. M.; List, N. H.; Martínez, T. J. Resolving the ultrafast dynamics of the anionic green fluorescent protein chromophore in water. *Chem. Sci.* **2021**, *12*, 11347–11363.
- (5) Zimmer, M. Green Fluorescent Protein (GFP): Applications, Structure, and Related Photophysical Behavior. *Chemical Reviews* **2002**, *102*, 759–782.
- (6) Jailaubekov, A. E.; Willard, A. P.; Tritsch, J. R.; Chan, W.-L.; Sai, N.; Gearba, R.; Kaake, L. G.; Williams, K. J.; Leung, K.; Rossky, P. J. et al. Hot charge-transfer excitons set the time limit for charge separation at donor/acceptor interfaces in organic photovoltaics. *Nature materials* 2013, 12, 66–73.

- (7) Nelson, T. R.; White, A. J.; Bjorgaard, J. A.; Sifain, A. E.; Zhang, Y.; Nebgen, B.; Fernandez-Alberti, S.; Mozyrsky, D.; Roitberg, A. E.; Tretiak, S. Non-adiabatic Excited-State Molecular Dynamics: Theory and Applications for Modeling Photophysics in Extended Molecular Materials. Chemical Reviews 2020, 120, 2215–2287.
- (8) Cofer-Shabica, D. V.; Menger, M. F. S. J.; Ou, Q.; Shao, Y.; Subotnik, J. E.; Faraji, S. INAQS, a Generic Interface for Nonadiabatic QM/MM Dynamics: Design, Implementation, and Validation for GROMACS/Q-CHEM simulations. *Journal of Chemical Theory and Computation* 2022, 18, 4601–4614.
- (9) Epifanovsky, E.; Gilbert, A. T. B.; Feng, X.; Lee, J.; Mao, Y.; Mardirossian, N.; Pokhilko, P.; White, A. F.; Coons, M. P.; Dempwolff, A. L. et al. Software for the frontiers of quantum chemistry: An overview of developments in the Q-Chem 5 package. The Journal of Chemical Physics 2021, 155, 084801.
- (10) Frisch, M. J.; Trucks, G. W.; Schlegel, H. B.; Scuseria, G. E.; Robb, M. A.; Cheeseman, J. R.; Scalmani, G.; Barone, V.; Petersson, G. A.; Nakatsuji, H. et al. Gaussian 16 Revision B.01. 2016; Gaussian Inc. Wallingford CT.
- (11) Plasser, F.; Ruckenbauer, M.; Mai, S.; Oppel, M.; Marquetand, P.; González, L. Efficient and Flexible Computation of Many-Electron Wave Function Overlaps. *J. Chem. Theory Comput.* **2016**, *12*, 1207–1219.
- (12) Avagliano, D.; Bonfanti, M.; Garavelli, M.; González, L. QM/MM nonadiabatic dynamics: the SHARC/COBRAMM approach. J. Chem. Theory Comput. 2021, 17, 4639–4647.
- (13) Bondanza, M.; Demoulin, B.; Lipparini, F.; Barbatti, M.; Mennucci, B. Trajectory Surface Hopping for a Polarizable Embedding QM/MM Formulation. J. Phys. Chem. A 2022, 126, 6780–6789.

- (14) Lindh, R.; González, L. Quantum Chemistry and Dynamics of Excited States: Methods and Applications; John Wiley & Sons, 2020; Chapter 16, pp 499–530.
- (15) Mai, S.; Marquetand, P.; González, L. Nonadiabatic dynamics: The SHARC approach.

  Wiley Interdisciplinary Reviews: Computational Molecular Science 2018, 8, e1370.
- (16) Jasper, A. W.; Truhlar, D. G. In Conical Intersections: Theory, Computation and Experiment; Domcke, W., Yarkony, D. R., Koppel, H., Eds.; World Scientific Publishing Co.: New Jersey, 2011; pp 375–414.
- (17) Tully, J. C. Molecular dynamics with electronic transitions. J. Chem. Phys. 1990, 93, 1061–1071.
- (18) Jain, A.; Alguire, E.; Subotnik, J. E. An Efficient, Augmented Surface Hopping Algorithm That Includes Decoherence for Use in Large-Scale Simulations. *Journal of Chemical Theory and Computation* **2016**, *12*, 5256–5268.
- (19) Belyaev, A. K.; Lasser, C.; Trigila, G. Landau–Zener type surface hopping algorithms. *J. Chem. Phys.* **2014**, *140*, 224108.
- (20) Miertuš, S.; Scrocco, E.; Tomasi, J. Electrostatic interaction of a solute with a continuum. A direct utilizaion of AB initio molecular potentials for the prevision of solvent effects. *Chem. Phys.* **1981**, *55*, 117–129.
- (21) Senn, H. M.; Thiel, W. QM/MM methods for biomolecular systems. *Angew. Chem.* **2009**, 48, 1198–1229.
- (22) Mennucci, B. Polarizable continuum model. WIRES Comput. Mol. Sci. 2012, 2, 386–404.
- (23) Groenhof, G. In *Biomolecular Simulations: Methods and Protocols*; Monticelli, L., Salonen, E., Eds.; Humana Press: Totowa, NJ, 2013; pp 43–66.

- (24) Viquez Rojas, C. I.; Slipchenko, L. V. Exchange repulsion in quantum mechanical/effective fragment potential excitation energies: Beyond polarizable embedding. Journal of Chemical Theory and Computation 2020, 16, 6408–6417.
- (25) Shao, Y.; Head-Gordon, M.; Krylov, A. I. The spin–flip approach within time-dependent density functional theory: Theory and applications to diradicals. *The Journal of chemical physics* **2003**, *118*, 4807–4818.
- (26) Caleman, C.; van Maaren, P. J.; Hong, M.; Hub, J. S.; Costa, L. T.; van der Spoel, D. Force Field Benchmark of Organic Liquids: Density, Enthalpy of Vaporization, Heat Capacities, Surface Tension, Isothermal Compressibility, Volumetric Expansion Coefficient, and Dielectric Constant. *Journal of Chemical Theory and Computation* 2012, 8, 61–74.
- (27) Sami, S.; Menger, M. F.; Faraji, S.; Broer, R.; Havenith, R. W. A. Q-Force: Quantum Mechanically Augmented Molecular Force Fields. *Journal of Chemical Theory and Computation* **2021**, *17*, 4946–4960.
- (28) Polyak, I.; Hutton, L.; Crespo-Otero, R.; Barbatti, M.; Knowles, P. J. Ultrafast Photoinduced Dynamics of 1,3-Cyclohexadiene Using XMS-CASPT2 Surface Hopping. *Journal of Chemical Theory and Computation* 2019, 15, 3929–3940.
- (29) Liu, P.; Agrafiotis, D. K.; Theobald, D. L. Fast determination of the optimal rotational matrix for macromolecular superpositions. *Journal of computational chemistry* 2010, 31, 1561–1563.
- (30) Theobald, D. L. Rapid calculation of RMSDs using a quaternion-based characteristic polynomial. Acta Crystallographica Section A: Foundations of Crystallography 2005, 61, 478–480.
- (31) Pechukas, P. Time-Dependent Semiclassical Scattering Theory. II. Atomic Collisions. *Physical Review* **1969**, *181*, 174–185.

- (32) Herman, M. F. Nonadiabatic semiclassical scattering. I. Analysis of generalized surface hopping procedures. *Journal of Chemical Physics* **1984**, *81*, 754–763.
- (33) Kapral, R.; Ciccotti, G. Mixed quantum-classical dynamics. The Journal of Chemical Physics 1999, 110, 8919–8929.
- (34) Nielsen, S.; Kapral, R.; Ciccotti, G. Mixed quantum-classical surface hopping dynamics.

  The Journal of Chemical Physics 2000, 112, 6543–6553.
- (35) Subotnik, J. E.; Ouyang, W.; Landry, B. R. Can we derive Tully's surface-hopping algorithm from the semiclassical quantum Liouville equation? Almost, but only with decoherence. *The Journal of chemical physics* **2013**, *139*, 211101.
- (36) Mai, S.; Marquetand, P.; González, L. Nonadiabatic Dynamics: The SHARC Approach. WIREs Comput. Mol. Sci. 2018, 8, e1370.
- (37) Parandekar, P. V.; Tully, J. C. Mixed quantum-classical equilibrium. *Journal of Chemical Physics* **2005**, *122*, 094102.
- (38) Schmidt, J. R.; Parandekar, P. V.; Tully, J. C. Mixed quantum-classical equilibrium: Surface hopping. *Journal of Chemical Physics* **2008**, *129*, 044104.
- (39) Jasper, A. W.; Truhlar, D. G. Improved treatment of momentum at classically forbidden electronic transitions in trajectory surface hopping calculations. *Chemical Physics Letters* **2003**, *369*, 60–67.
- (40) Coffman, A. J.; Jin, Z.; Chen, J.; Subotnik, J. E.; Cofer-Shabica, D. V. On the use of QM/MM Surface Hopping simulations to understand thermally-activated rare event nonadiabatic transitions in the condensed phase. *Journal of Chemical Theory and Computation* **2023**, In press.

# TOC Graphic

